REGULAR ARTICLE

blood advances

ETS1 is a novel transcriptional regulator of adult T-cell leukemia/lymphoma of North American descent

Rebecca A. Luchtel,[1] Yongmei Zhao,[2] Ritesh K. Aggarwal,[3] Kith Pradhan,[4] and Shahina B. Maqbool[2]

[1]Division of Hematology and Oncology, Department of Medicine, Northwestern University, Chicago, IL; and [2]Department of Genetics, [3]Department of Medicine, and [4]Department of Epidemiology & Population Health (Biostatistics), Albert Einstein College of Medicine, Bronx, NY

Key Points

- The ETS1 DNA binding motif is enriched in open chromatin of NA-ATLL compared with J-ATLL cell lines.
- ETS1 drives cell growth and *CCR4* expression in NA-ATLL.

Adult T-cell leukemia/lymphoma (ATLL) is an aggressive T-cell lymphoma associated with the human T-cell lymphotropic virus type 1 virus endemic in regions including Japan, the Caribbean islands, and Latin America. Although progress has been made to understand the disease, survival outcomes with current standard therapy remain extremely poor particularly in acute ATLL, underlying the need for better understanding of its biology and identification of novel therapeutic targets. Recently, it was demonstrated that ATLL of North American–descendent patients (NA-ATLL) is both clinically and molecularly distinct from Japanese-descendent (J-ATLL), with inferior prognosis and higher incidence of epigenetic-targeting mutations compared with J-ATLL. In this study, combined chromatin accessibility and transcriptomic profiling were used to further understand the key transcriptional regulators of NA-ATLL compared with J-ATLL. The ETS1 motif was found to be enriched in chromatin regions that were differentially open in NA-ATLL, whereas the AP1/IRF4 motifs were enriched in chromatin regions more open in J-ATLL. *ETS1* expression was markedly elevated in NA-ATLL in both cell line and primary tumor samples, and knockdown of *ETS1* in NA-ATLL cells resulted in inhibition of cell growth. *CCR4*, a previously identified oncogenic factor in ATLL, was found to be a direct ETS1 transcriptional target in NA-ATLL. As such, ETS1 provides an alternate mechanism to enhance *CCR4* expression/activity in NA-ATLL, even in the absence of activating *CCR4* mutations (*CCR4* mutations were identified in 4 of 9 NA-ATLL cases). Taken together, this study identifies ETS1 as a novel dominant oncogenic transcriptional regulator in NA-ATLL.

Introduction

T-cell lymphomas are a highly heterogeneous group of lymphomas with a generally poor response to standard therapy.[1] Adult T-cell leukemia/lymphoma (ATLL) is a rare T-cell lymphoma that occurs in 2% to 5% of individuals infected with the human T-cell lymphotropic virus type 1 (HTLV-1) retrovirus.[2,3] The acute and lymphomatous ATLL subtypes follow an aggressive clinical course with a dismal prognosis (overall survival $<$ 1 year) despite intensive chemotherapy, whereas the less common chronic and smoldering subtypes are more indolent with favorable response to antiviral therapy. ATLL cases occur predominantly in HTLV-1 endemic regions, such as Japan, the Caribbean islands, and Latin America. Within the United

Submitted 29 March 2022; accepted 30 May 2022; prepublished online on *Blood Advances* First Edition 8 June 2022; final version published online xxx 2022. https://doi.org/10.1182/bloodadvances.2022007725.

NA-ATLL cell line RNA sequencing data described in this paper are available through GEO (GSE205653).

The full-text version of this article contains a data supplement.

States, New York City has disproportionately high ATLL incidence as it hosts a large population of Caribbean-born immigrants.[4,5]

Recent work has illuminated clinical and molecular differences between ATLL arising in patients of Japanese (J-ATLL) compared with North American (NA-ATLL) descent. Epidemiologic and genomic analysis of NA-ATLL cohorts reported a younger median age of diagnosis (40-50 years), larger proportion of aggressive subtypes (acute and lymphomatous; ~90%), shorter overall survival (6 months), and greater frequency of epigenetic mutations (57%) compared with patients with ATLL born outside of North America.[4-9] However, despite disparate prognostic and mutation profiles, J-ATLL and NA-ATLL are currently treated similarly because of the limited understanding of NA-ATLL biology and pathogenesis.

ATLL cells generally express Treg phenotypic markers,[10-12] and tumorigenesis is thought to progress in HTLV-1–infected T cells through a series of epigenetic and genetic events.[13] Interactions between HTLV-1 viral proteins and the epigenome further support a role for epigenetics in ATLL pathogenesis. HTLV-1 encodes several viral proteins, of which Tax and HBZ are thought to be critically involved in clonal expansion of infected cells and subsequent oncogenesis.[14] Both Tax and HBZ interact with chromatin machinery to facilitate transcriptional and epigenetic alterations promoting tumorigenesis.[15,16] This was illustrated by a recent study showing that HBZ interacts with an ATLL-specific *BATF3* super enhancer to drive the BATF3/IRF4 transcriptional program that was critical to ATLL growth.[17]

However, epigenetic molecular profiling studies have been reported exclusively in J-ATLL models, whereas the epigenetic and transcriptional landscape of NA-ATLL remains unknown. Given the disproportionately high mutation rate of epigenetic regulators in NA-ATLL and the known role for chromatin regulation in ATLL pathogenesis, we sought to characterize chromatin accessibility and transcriptional regulation in NA-ATLL and compare it with J-ATLL. Combined assay for transposase-accessible chromatin (ATAC) and RNA sequencing on cell lines representing each subgroup demonstrated differential transcriptional regulation between J-ATLL and NA-ATLL. ETS1 was identified as a dominant and unique transcriptional regulator in NA-ATLL. We then confirmed expression and the oncogenic role of the transcription factor, ETS1, through analysis of primary tumor samples and in vitro assays.

Methods

Cell lines

NA-ATLL cell lines ATL13, ATL18, ATL21, and ATL29 were cultured in Iscove's Modified Dulbecco's Medium (IMDM) with 20% human serum (Valley Biomedical, Winchester, VA) and 100 U/mL interleukin 2 (IL2; BD Biosciences, San Jose, CA).[18] Japanese ATLL cell lines were cultured in RPMI 1640 with 10% fetal bovine serum (Gemini Bio-Products, West Sacaramento, CA) in the absence (ATL34Tb- and ED40515-) or presence (ATL43T+ and ED41214+) of 100 U/mL IL2.[19]

ATAC-seq

ATAC sample processing was performed on 25 000 cells per cell line by the Epigenomics Shared Facility at Albert Einstein College of Medicine using the Omni-ATAC protocol.[20] Normal healthy T-cell ATAC-seq data for T_{eff} ($CD4^+CD127^+$) and T_{reg} ($CD4^+CD25^+$) cells with and without stimulation were obtained from GSE118189[21] (supplemental Table 1). Sequencing and analysis were performed by Genewiz (South Plainfield, NJ). All data were trimmed using Trimmomatic 0.38, and cleaned reads aligned to reference genome hg38 using bowtie2.[22] Aligned reads were filtered using SAMtools 1.9,[23] and polymerase chain reaction (PCR) or optical duplicates were marked using Picard 2.18.26 and removed. Before peak calling, reads mapping to mitochondria were called and filtered, and reads mapping to unplaced contigs were removed. MACS2 2.1.2[24] was used for peak calling to identify open chromatin regions. Valid peaks from each group were merged, and peaks called in at least 66% of samples are kept for downstream analyses. For each pairwise comparison, peaks from each condition were merged and peaks found in either condition were kept for downstream analyses. Reads falling beneath peaks were counted in all samples, and these counts were used for differential peak analyses using the R package Diffbind (Stark and Brown[25]). DiffBind was used for differential region of interest detection using a false discovery rate (FDR) ≤ 0.05 as a cutoff.

Motif analysis

Motif discovery was performed on cell line and normal T-cell ATAC-seq data. Top differentially accessible regions were filtered by (adjusted $P < .05$; fold change (fc) > 2) from each comparison using the MEME Suite[26] tools: MEME-ChIP[27] and DREME. Transcription factor binding prediction was performed using Tomtom[28] against the JASPAR and ETS factors motif databases. Find Individual Motif Occurences (FIMO) was used to determine the percent of total sequences containing a given motif ($P < .001$), and Analysis of Motif Enrichment (AME) was used to determine the difference in motif enrichment between two groups (Fisher's exact test).

RNA-sequencing and microarray transcriptome analysis

Datasets and sample sources used in transcriptome analyses are listed in supplemental Table 1. Cell line RNA was isolated using Qiagen RNAeasy (Qiagen). RNA sequencing libraries were prepared using Stranded mRNA kit (Illumina). Sequencing (150 bp, paired end) and analysis was performed by Genewiz. Normal T-cell RNA sequencing data paired to ATAC-seq for normal T cells were obtained from GSE118165.[21] For both cell line and normal T-cell samples, sequence reads were trimmed to remove possible adapter sequences and nucleotides with poor quality using Trimmomatic v.0.36. The trimmed reads were mapped to the *Homo sapiens* GRCh38 reference genome using the STAR aligner v.2.5.2b. Unique gene hit counts were calculated by using featureCounts from the Subread package v.1.5.2. Comparison of gene expression between sample groups was performed using DESeq2, and the Wald test was used to generate P values and $\log_2$ fold changes. RNA isoforms were visualized in IGV software (Broad Institute). NA-ATLL patient and normal donor peripheral blood mononuclear cell (PBMC) RNA-sequencing data were previously published,[8] and differential analysis was performed using DESeq2. J-ATLL and normal CD4 T cell microarray data were accessed through GSE33615,[29,30] and data were analyzed using GEO2R.

Gene set enrichment and pathway analysis

Gene set enrichment analysis (GSEA) was performed as previously described.[31] Briefly, genes were ranked for each comparison using the product of $-\log(P \text{ value})$ and the sign of fold change. The

ranked dataset was then analyzed for enrichment of Hallmark and custom datasets using GSEA software (Broad Institute).[32] ETS1 target genes were defined by the TRANSFAC curated transcription factor targets gene set for ETS1 (Harmonizome[33,34]), as well as a recently published ETS1 target dataset in T-ALL.[35] Pathway analysis was performed on ETS1 target genes overexpressed in NA-ATLL compared with J-ATLL (fc > 0.5) and normal control cells (fc > 0.5; $P < .1$) using Ingenuity Pathway Analysis (IPA; Qiagen) software.

Mutation analysis

Mutations were detected in the previously published NA-ATLL RNA-seq dataset.[8] SNP/INDEL analysis was performed using mpileup within the Samtools v.1.3.1 program followed by VarScan v.2.3.9. The parameters for variant calling were as follows: minimum frequency of 25%, $P < .05$, minimum coverage of 10, and minimum read count of 7. Manual review of mapped reads within the region of interest was also performed.

Chromatin immunoprecipitation

Chromatin immunoprecipitation sequencing (ChIP-seq) data for T-regulatory (Treg) cells were accessed through GSE43119 and the FANTOM5 project https://fantom.gsc.riken.jp/data/.[36] H3K27ac, H3K4me1, and ETS1 ChIP-seq tracks were visualized using the UCSC Genome Browser. ETS1 ChIP-seq data for Jurkat cells were accessed through GSE17954.[37]

Enhancer annotation

Human ACtive Enhancer to interpret Regulatory variants (HACER) was used to annotate genomic coordinates with chromatin interactions and enhancer information.[38] Identification of enhancers overlapping with specific genomic coordinates was assessed from Cap Analysis of Gene Expression data derived from a large range of cell types including T cells. Enhancer target genes were determined by FANTOM5 project.[39]

Gene model

Illustrator for Biological Sequences (GPS[40]) was used to construct the *ETS1* and *CCR4* gene models.

siRNA knockdown

Small interfering RNA (siRNA) targeting *ETS1* or nontarget control (ON-TARGETplus SMARTpool, Dharmacon) was transfected by electroporation using Amaxa Nucleofector II (Lonza). Cells were harvested for functional assays, and knockdown efficiency was assessed by quantitative PCR (qPCR) 48 or 72 hours after transfection.

Cell viability

Equal number of viable cells were plated 24 hours after transfection. Cell viability was determined 48 to 72 hours after transfection using the CellTiter-Blue Cell Viability Assay (Promega).

Western blotting

Western blotting was performed on protein lysates as previously described.[41] The following primary antibodies were used to detect proteins of interest: ETS1 (Proteintech, 66598-1-IG) and β-actin (Novus, NB600-501). Total protein was visualized using Revert Total Protein stain (Li-Cor). Proteins were visualized using Li-Cor IR-dye secondary antibodies on an Odyssey FC Imaging System (Li-Cor).

qPCR

RNA was isolated using Qiagen RNAeasy (Qiagen) and reverse transcribed to cDNA using SuperScript III First-Strand Synthesis SuperMix (Invitrogen). qPCR was performed using EvaGreen qPCR Mastermix (Applied Biologic materials Inc) with the following primer sequences: *ETS1* forward: GGCAGTTTCTTCTGGAATTA, *ETS1* reverse: CACGGCTCAGTTTCTCATA[42]; *CCR4* forward: CTCTGGCTTTTGTTCACTGCTGC, *CCR4* reverse: AGCCCA CAGTATTGGCAGAGCA (Origene), *ACTB* forward: CATCCT GCGTCTGGACCT, *ACTB* reverse: TAATGTCACGCACGAT TTCC.[43] Results were normalized using *ACTB* and relative fold change was calculated using the ΔΔCt method.

Statistical analyses

Statistical analysis was performed using the Student *t* test (in vitro data) or univariate generalized linear model (GLM) models, as indicated, through SPSS (IBM, Armonk, NY) and JMP (SAS Institute Inc., Cary, NC) software. *P* values are adjusted for multiple testing where indicated in ATAC-sequencing, RNA-sequencing, and microarray comparisons.

Results

NA-ATLL and J-ATLL have distinct chromatin accessibility profiles

To identify and compare chromatin accessibility profiles between NA-ATLL and J-ATLL, ATAC-sequencing was performed on 8 ATLL cell lines (4 NA-ATLL: ATL13, ATL18, ATL21, and ATL29; and 4 J-ATLL: ATL34Tb-, ED40515-, ATL43T+, and ED41214+) and compared with chromatin accessibility of regulatory $CD4^+$ T cells (Treg; $CD4^+CD25^+$) and effector $CD4^+$ T cells ($CD4_{EF;}$ $CD4^+CD127^+$) derived from healthy controls. The cell lines were chosen to represent the mutational spectrum of ATLL including mutations targeting JAK/STAT, *TP53*, *EP300*/epigenetic, and immune-related genes.[8] Unsupervised clustering showed that ATLL cell lines clustered separately from normal cells (supplemental Figure 1A). In addition, NA-ATLL cell lines clustered separately from J-ATLL cell lines with the exception of the J-ATLL cell line, ATL-43T+, which clustered with NA-ATLLs. ATL-43T+ was retained in the J-ATLL group for all comparisons. Chromatin accessibility of stimulated T_{reg} and $CD4_{EFF}$ cells were more closely correlated to ATLLs than unstimulated T cells (supplemental Figure 1A). Because ATLL is known to have a T_{reg}-like immunophenotype, we chose stimulated Tregs as the normal control for subsequent comparisons.

Differentially accessible regions in NA-ATLL and J-ATLL have unique motif enrichment

Analysis of genes annotated to chromatin accessibility peaks, showed significant overlap between ATLL cell lines and stimulated Treg samples (72.8%). However, NA-ATLL and J-ATLL chromatin accessibility also mapped to 1,348 and 2,051 unique genes, respectively. Given these differences in global chromatin accessibility between NA-ATLL and J-ATLL, we investigated transcription factor binding motif enrichment in differentially accessibility regions. Differentially accessible regions between NA-ATLL and J-ATLL (n = 3876 regions) were mapped predominantly to gene promoters (29%), intronic (37%), and distal intergenic regions (28%; supplemental Figure 1B). Of the regions that were more accessible in NA-ATLL cell lines, the most

significantly enriched motif, AGGAAGW, corresponded to the ETS family of transcription factors (Figure 1A). Based on prediction score and expression of ETS transcription factors predicted to bind to this sequence, ETS proto-oncogene 1 (ETS1) was presumed to be the dominant ETS transcription factor recognizing the enriched ETS motif in NA-ATLL (supplemental Table 2). This motif was also significantly more enriched in total NA-ATLL chromatin accessibility peaks compared with Treg and J-ATLL (Figure 1B). When restricted to promoter regions (2 kb ± TSS), enrichment of the RUNX1 motif was also identified in sites with increased accessibility in NA-ATLL (E-value = 0.029); however, the RUNX1 motif was not enriched in total NA-ATLL peaks compared with J-ATLL (supplemental Figure 2A). Of note, RUNX1 has been shown to interact with ETS1.[44]

In contrast, the chromatin regions with greater accessibility in J-ATLL cell lines were enriched in 4 motifs, of which AP1 and IRF4 motifs were the most significantly enriched (Figure 1A; suppl Figure 2C). These motifs were also enriched in total J-ATLL accessible regions

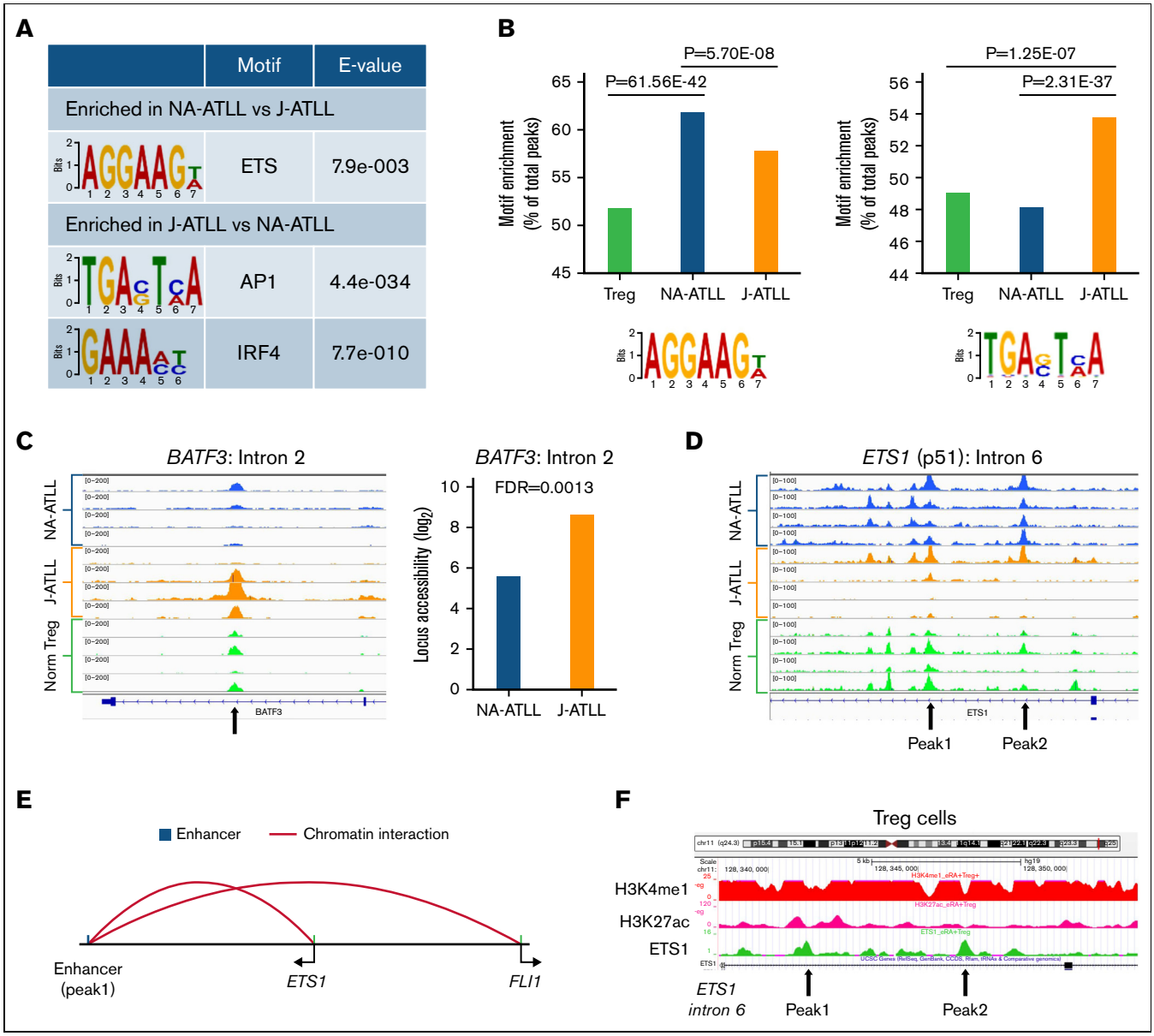

Figure 1. NA-ATLL and J-ATLL have differentially enriched motifs in accessible chromatin regions. (A) Motif enrichment in differentially accessible regions between NA-ATLL (n = 4) and J-ATLL (n = 4) cell lines. ETS1 motif was significantly enriched in chromatin regions that were more accessible in NA-ATLL cell lines, whereas AP1 and IRF4 motifs were enriched in chromatin regions that were more accessible in J-ATLL cell lines. (B) Comparison of overall enrichment of ETS1 and AP1 motifs (percent of total peaks containing the motif) across normal Treg cells and NA-ATLL and J-ATLL cell lines. The ETS1 motif is significantly enriched in NA-ATLL cell line peaks and the AP1 motif is significantly enriched in J-ATLL cell line peaks. (C) J-ATLL cell lines have significantly greater chromatin accessibility (FDR = 0.0013) at the *BATF3* intronic region (intron 2) overlapping with a previously identified HBZ binding site.[17] (D) Two intronic peaks in *ETS1* (intron 6) were accessible primarily in NA-ATLL cell lines. (E) Intron 6 peak 1 has been identified as an enhancer for *ETS1* and the ETS family member *FLI1* through direct chromatin interaction (FANTOM5[39]). (F) ETS1 accessible peaks identified by ATAC-seq overlap with ETS1 binding sites in Treg ETS1 ChIP-seq.

compared with NA-ATLL and Treg cells (Figure 1B; supplemental Figures 2B and 3). This is consistent with a recent report in J-ATLL cell lines in which HBZ was shown to interact with the AP1 member, BATF3, and its heterodimer partner, IRF4. In this study, HBZ was shown to interact at the *BATF3* locus superenhancer, driving expression of *BATF3* and the downstream BATF3-IRF4 transcriptional program.[17] Indeed, we observed chromatin accessibility of the same *BATF3* intronic site in 3 of the 4 J-ATLL cell lines and significantly greater accessibility of this site in J-ATLL cell lines compared with NA-ATLL (FDR = 0.0013; Figure 1C). We then determined whether the *ETS1* locus also had differential chromatin accessibility. Like *BATF3*, *ETS1* contained differentially accessible intronic regions (Figure 1D). Peak 1 corresponds to a previously identified intronic enhancer that interacts with ETS1 (Figure 1E). Motif analysis of these regions identified enrichment of the ETS1 motif. Consistent with this, these regions are characterized by H3K3me1 and ETS1 binding in Treg ChIP seq[36] (Figure 1F) and ETS1 binding in Jurkat ChIP-seq[37] (supplemental Figure 4).

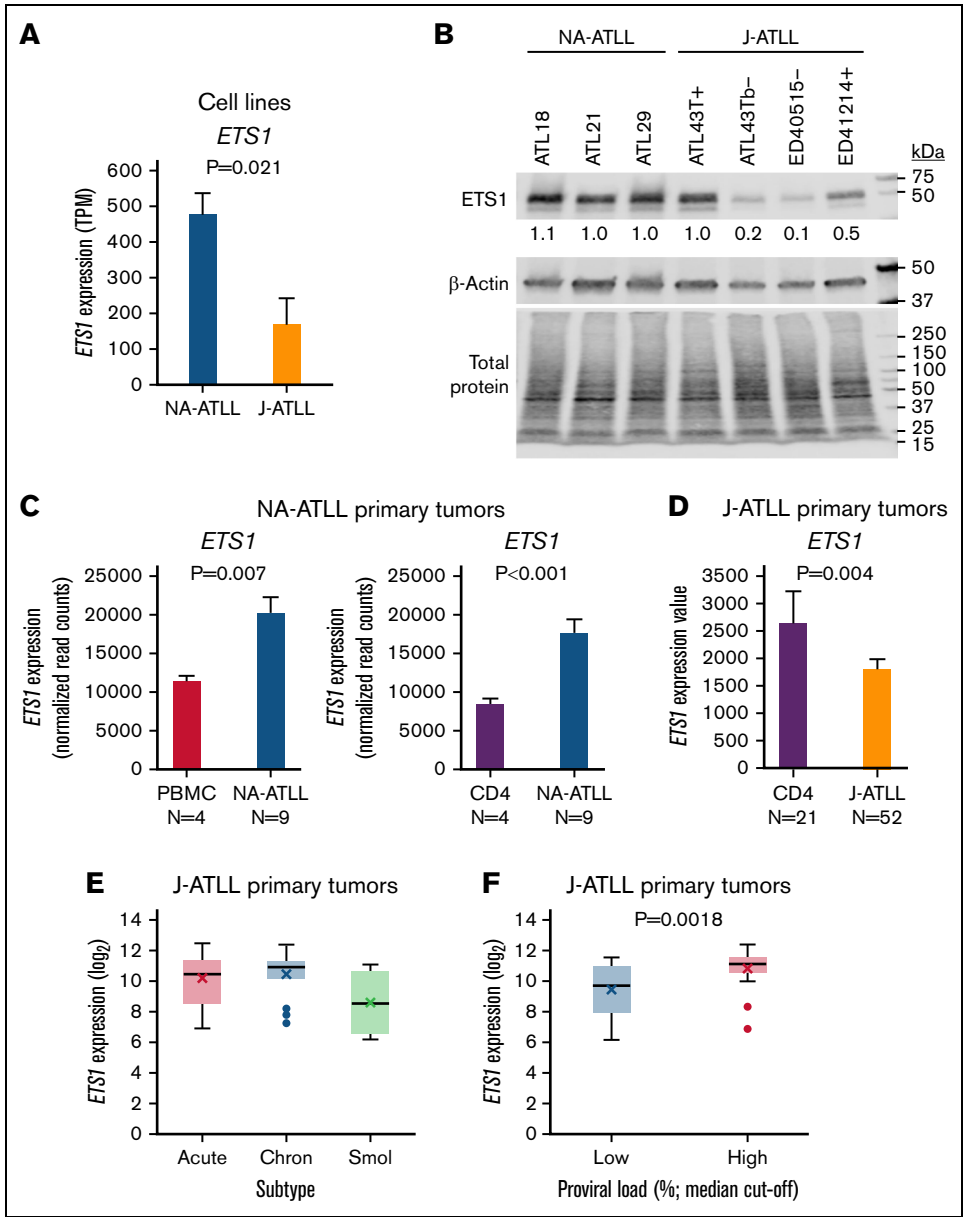

Figure 2. ETS1 expression is upregulated in NA-ATLL cell line and primary tumor cells. (A) RNA-seq *ETS1* expression in NA-ATLL (n = 4) compared with J-ATLL (n = 4) cell lines. Mean ± standard error (SE); 2-sided *t* test; TPM, transcripts per million. (B) Western blot validation of ETS1 expression across ATLL cell lines. ETS1 relative abundance is normalized to total protein. (C) *ETS1* expression is elevated in NA-ATLL primary tumor cells compared with PBMCs and CD4 T cells derived from healthy donors. RNA-seq; mean normalized read counts ± SE; FDR-corrected *P* value. (D) *ETS1* expression in J-ATLL primary tumor cells compared with healthy donor CD4 cells. FDR-corrected *P* value. (E) *ETS1* expression across ATLL subtypes (*P* = .113). Chron, Chronic; Smol, Smoldering. (F) *ETS1* expression stratified by low and high proviral load (median cutoff: proviral load 78.4%, *P* = .0018).

ETS1 is overexpressed in NA-ATLL

We then assessed RNA-sequencing data to determine the expression of these transcription factors in cell lines. *ETS1* expression was significantly elevated in NA-ATLL cell lines compared with J-ATLL cell lines (2.8-fold; $P = .02$; Figure 2A) and was not increased by stimulation status in normal T cells (supplemental Figure 5). Analysis of transcriptome data showed the dominant isoform of *ETS1* to be p51 (NM_005238; supplemental Figure 6) across all cell lines, and no nonsynonymous mutations or intron retention events were identified in *ETS1*. Cell line expression of ETS1 was confirmed by Western blot, with similar degree of upregulation in NA-ATLL ($P = .03$; Figure 2B; supplemental Figure 7).

To confirm the differential regulation of *ETS1* expression between NA-ATLL and J-ATLL, we analyzed primary tumor gene expression data. In PBMCs isolated from 9 patients with NA-ATLL and 4 healthy controls, *ETS1* expression was significantly elevated in NA-ATLL (Figure 2C[8]). Similar findings were observed in the comparison between NA-ATLL and healthy donor CD4 T cells (Figure 2C; logfc = 10.6; FDR < 0.001). In contrast, analysis of gene expression dataset of 52 J-ATLL tumors compared with healthy donor CD4 T cells showed downregulation of *ETS1*[29,30] (Figure 2D). Subtype distribution is known to differ between NA-ATLL and J-ATLL; therefore, we compared *ETS1* across subtypes in the J-ATLL dataset. *ETS1* expression was similarly downregulated in J-ATLL Acute subtype compared with CD4 T cells (supplemental Figure 8), and there were no subtype-specific differences in *ETS1* expression between acute (N = 26), chronic (N = 20), and smoldering (N = 4) in a univariate analysis ($P = .113$; Figure 2E). There were insufficient numbers of each subtype for comparison within the NA-ATLL dataset (acute, N = 8; chronic/smoldering, N = 1). Given the previously shown association of ETS1 with the HTLV-1 viral protein, Tax, we segregated tumors into low and high proviral load (median cutoff) and compared expression of *ETS1*. Notably, *ETS1* expression was higher ($P = .0018$) in the high proviral load subset (Figure 2F). Although the trend was maintained, significance was lost when comparing *ETS1* between low and high proviral loads within the J-ATLL acute subtype (supplemental Figure 8B).

Primary tumor expression also supported the upregulation of *BATF3* in J-ATLL (supplemental Figure 9A). *BATF3* was not different between NA-ATLL in PBMCs isolated from NA-ATLL patients and healthy controls but was significantly elevated in J-ATLL primary tumor cells compared with control CD4 cells (supplemental Figure 9B-C). Unlike *ETS1*, *BATF3* was found to be significantly elevated in acute compared with smoldering ATLL subsets in a J-ATLL cohort (supplemental Figure 9D). In addition, *BATF3* expression was slightly elevated in J-ATLLs with high vs low proviral load ($P = .011$; supplemental Figure 9E); however, this trend was lost when analyzed within the acute subtype only (data not shown). Together, these data support disparate transcriptional regulators between J-ATLL and NA-ATLL.

ETS1 promotes cell growth, migration, and adhesion in NA-ATLL

We next sought to characterize the function of ETS1 in NA-ATLL. ETS1 has been shown to act as an oncogene, promoting proliferation, invasiveness, migration, and chemoresistance in many tumor types, including lymphomas.[45-47] GSEA confirmed upregulation of ETS1 target genes in NA-ATLL compared with J-ATLL (Figure 3A). Pathway analysis of ETS1 target genes upregulated in NA-ATLL identified lymphocyte proliferation as a top pathway (Figure 3B). To functionally assess the role of ETS1 in proliferation, siRNA-mediated knockdown of *ETS1* was performed in NA-ATLL cell lines (supplemental Figure 10). Knockdown of *ETS1* in ATL18, ATL21, and ATL29 cell lines resulted in 0.47-, 0.51-, and 0.57-fold cell growth relative to control siRNA cells, respectively (Figure 3C-E).

CCR4 is a transcriptional target of ETS1 in NA-ATLL

To identify potential target genes of ETS1 in NA-ATLL, we focused on genes experimentally demonstrated to be direct ETS1 target genes that were upregulated in NA-ATLL cell lines compared with J-ATLL cell lines (fc > 0.5) and in NA-ATLL primary tumor cells compared with normal PBMC/CD4 cells (log fc > 0.5; FDR < 0.1). For ETS1 target genes that were consistently upregulated in each comparison, we then assessed chromatin accessibility to identify genes with differential chromatin accessibility in NA-ATLL compared with J-ATLL cells. *CCR4* was a primary candidate gene identified by this approach.

A region of chromatin accessibility was identified exclusively in NA-ATLL overlapping the *CCR4* TSS and containing multiple predicted ETS1 binding sites (Figure 4A-B). ETS1 has been shown to bind to the *CCR4* TSS by ChIP-seq in Treg cells (Figure 4C) and Jurkat cells (supplemental Figure 11).

CCR4 gene expression was found to be significantly elevated in NA-ATLL compared with J-ATLL cell lines and in NA-ATLL primary compared with normal CD4 T cells (Figure 4D). Moreover, a strong correlation was observed between *CCR4* and *ETS1* gene expression in both cell lines and primary tumor cells (Figure 4E). Together with chromatin accessibility encompassing ETS1 binding sites and demonstrated binding of ETS1 to the *CCR4* TSS, these data strongly indicate *CCR4* as a direct transcriptional target in NA-ATLL. To confirm this relationship in NA-ATLL, we assessed *CCR4* expression after *ETS1* knockdown and observed significant inhibition of *CCR4* expression with loss of *ETS1* in NA-ATLL cell lines (Figure 4F).

GATA3 has been previously implicated as driver of *CCR4* in J-ATLL[48] and along with ETS1 has several DNA binding motifs in the *CCR4* promoter region. Although *GATA3* is elevated in NA-ATLL primary tumor compared with control cells, it is not correlated with *CCR4* expression in NA-ATLL primary tumors ($R^2 = -0.14$; $P = .85$; supplemental Figure 12). In contrast, and consistent with the prior reports in J-ATLL, *GATA3* is strongly correlated with *CCR4* expression in J-ATLL primary tumors ($R^2 = 0.54$; $P < .001$; supplemental Figure 12).

CCR4 is a well-characterized oncogene in J-ATLL that is recurrently mutated in ~30% of J-ATLL.[49] Expression of mutant *CCR4* resulted in decreased receptor internalization in response to ligand[50] and increased migration toward its ligands CCL17 and CCL22.[49]

However, mutational status of *CCR4* in NA-ATLL has not been reported previously. We assessed *CCR4* mutation status in NA-ATLL cell lines from RNA-sequencing data. All 4 NA-ATLL cell lines lacked *CCR4* mutations (in contrast, exon 2 mutations have been reported in the 4 J-ATLL cell lines previously[49]). We then used NA-ATLL patient RNA sequencing data (n = 9) to identify *CCR4* exon 2 variants in this population. Similar to the frequency observed in J-ATLL, early stop/non-sense mutations in exon 2 were observed

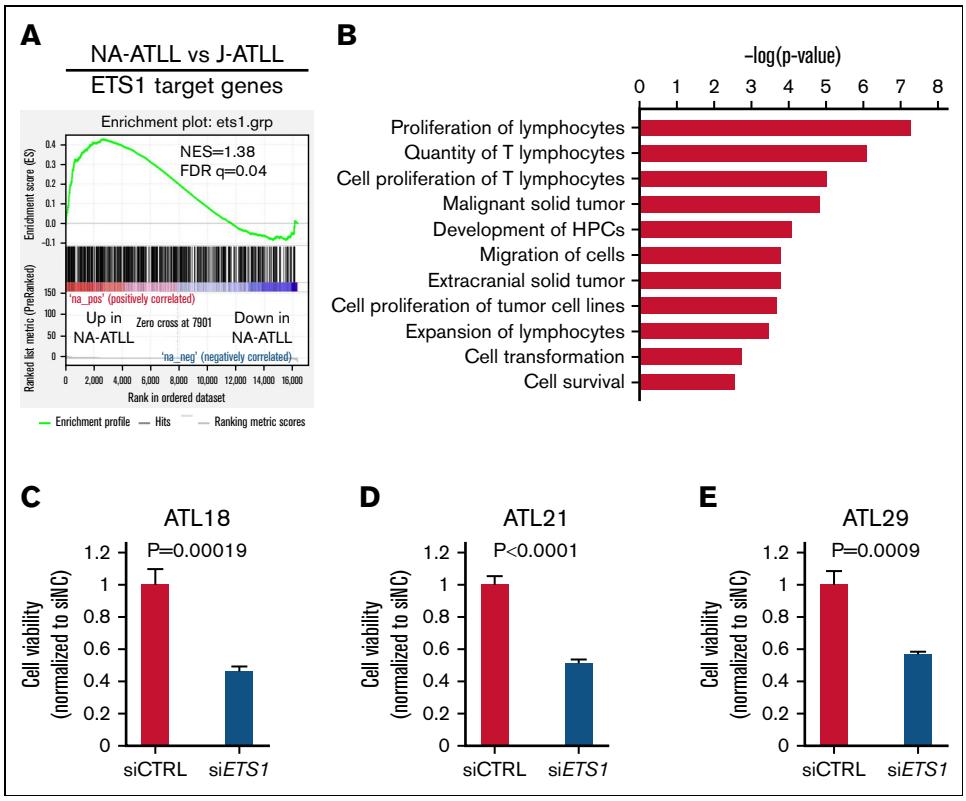

Figure 3. ETS1 drives cell growth in NA-ATLL. (A) Genes were ranked from most upregulated to most downregulated in NA-ATLL compared with J-ATLL cell lines. ETS1 target genes were significantly enriched in genes upregulated in NA-ATLL cell lines. (B) IPA pathway analysis of ETS1 target genes upregulated in NA-ATLL cell lines compared with J-ATLL cell lines and NA-ATLL primary tumor cells compared with normal PBMC and CD4 cells. (C-E) NA-ATLL cell lines ATL18, ATL21, and ATL29 were transfected with siRNA targeting *ETS1* or nontarget control. Equal number of viable cells were plated 24 hours after transfection, and relative cell number was determined by Cell Titer Blue assay at 48 hours (ATL18 and ATL21) or 72 hours (ATL29) after transfection. Two-sided *t* test, mean ± SE. Data shown are representative of 2 to 3 independent transfection experiments per cell line. Knockdown of *ETS1* gene expression was assessed by qPCR (supplemental Figure 10).

in 3 of the 9 cases (33%; supplemental Table 3). All 3 of these nonsense mutations were located in the C-terminal cytoplasmic region of the CCR4 protein. Two of these sites have been previously reported in ATLL (C329* and Y331*). In addition to these early stop mutations, a missense mutation was also identified in exon 2, I226F (c.928A>T), in the transmembrane region. Functional implications of this mutation are unknown, and it has not been previously reported in the COSMIC or dbSNP databases. Germline and tumor DNA were not available to confirm variant calls in these cases.

Expression of both *ETS1* and *CCR4* at the RNA level was higher in wild-type (n = 5) compared with mutated *CCR4* cases (n = 4; Figure 4G-H, *ETS1*, $P = .039$; *CCR4*, $P = .052$). Put together, these data suggest that ETS1 transcriptional regulation of *CCR4* may represent an alternate mechanism to enhance CCR4 expression/activity in NA-ATLL, in the absence of gain of function *CCR4* mutations.

Discussion

We report for the first time that chromatin accessibility of NA-ATLL is characterized by enrichment of ETS binding motifs and corresponding upregulation of *ETS1* expression. Disparate chromatin accessibility was observed between J-ATLL and NA-ATLL cells with the BATF3/IRF4 pathway identified as a primary transcriptional regulator in J-ATLL. Analysis of primary tumor RNA sequencing data in both NA-ATLL and J-ATLL cohorts confirmed that *ETS1* is elevated in NA-ATLL tumor cells compared with normal controls, whereas *ETS1* expression is lower in J-ATLL compared with normal T cells. Functional assays revealed that ETS1 drives cell growth in NA-ATLL and is a direct transcriptional regulator for *CCR4*. Together, these data provide further support for NA-ATLL as a distinct entity with a unique molecular profile characterized by aberrant expression of *ETS1* and identify ETS1 as a key transcriptional regulator of in NA-ATLL.

ETS1 is an Ets family transcription factor expressed in multiple cell types, including T lymphocytes. Mice deficient for Ets1 have demonstrated a critical role for Ets1 in Treg development and function.[51] Overexpression, association with poor prognosis, and oncogenic function of ETS1 has been shown in multiple malignancies.[52] In PTCL, ETS1 expression has been reported to varying degrees across several subtypes, with the highest observed in extranodal NK/TCL and weaker positive staining in AITL and ALCL.[53,54] In a Chinese population of PTCLs, ETS1 expression was not significantly associated with outcome, although ATLL cases were not included in this study.[54]

ETS1 has been shown to interact with the HTLV-1 viral protein, Tax,[55,56] and to cooperate with Tax to transactivate target genes.[57] Moreover, ETS1 has been shown to bind and activate the HTLV-1 LTR, providing a possible mechanism for activation of latent

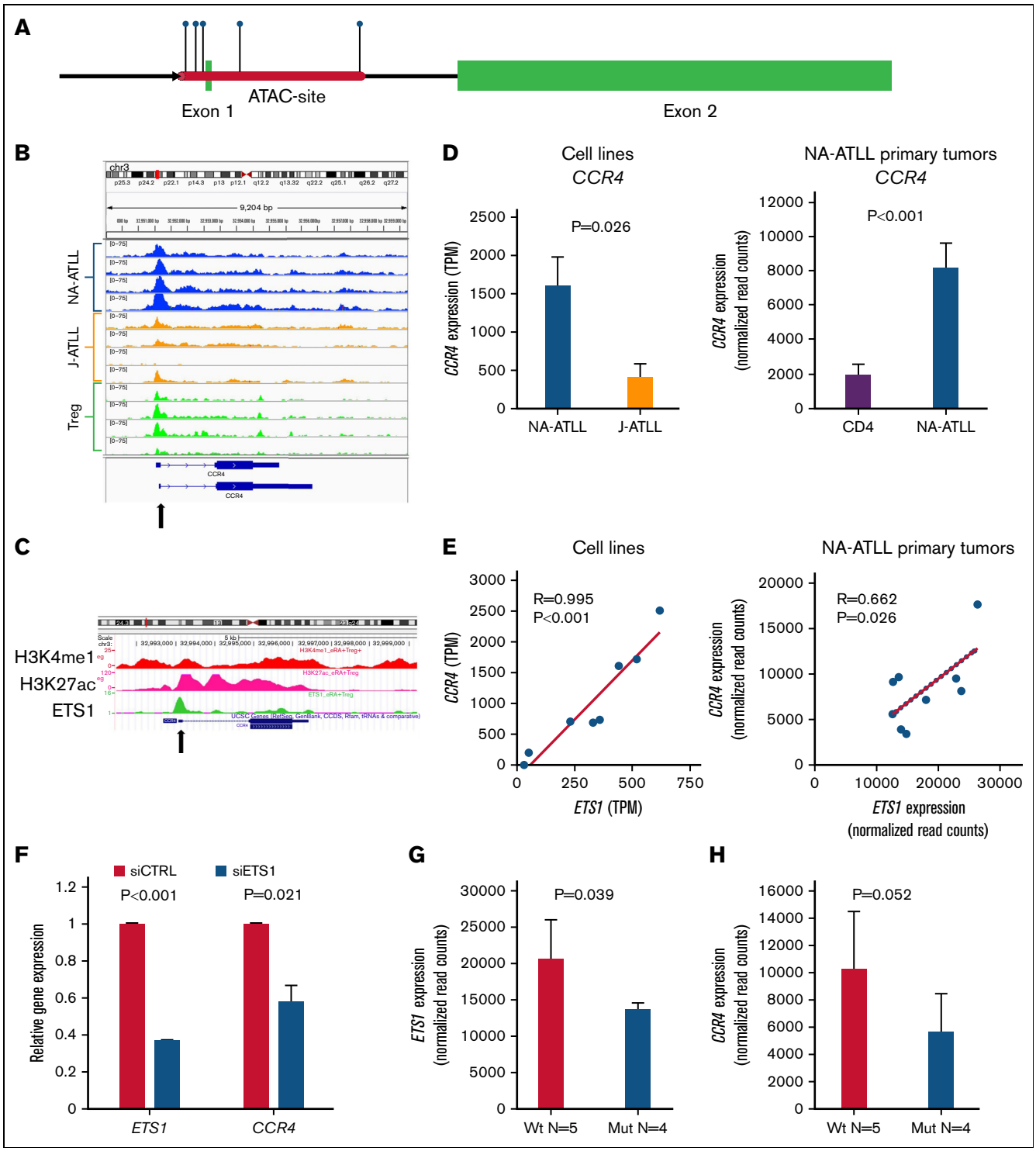

Figure 4. *CCR4* is a transcriptional target of ETS1 in NA-ATLL. (A) *CCR4* gene map of chromatin accessibility and ETS1 binding motifs. Purple, NA-ATLL specific chromatin accessibility (ATAC-seq); Lollipops, predicted ETS1 binding sites within open chromatin region; Green, exons. (B) NA-ATLL–specific chromatin accessibility over *CCR4* TSS region. ATAC-seq data shown for NA-ATLL, J-ATLL, and normal Treg cells. (C) ETS1 binding to the *CCR4* promoter region corresponding to chromatin accessibility site was confirmed by analysis of ETS1 ChIP-seq data in Treg cells. (D) *ETS1* expression in NA-ATLL and J-ATLL cell lines (mean ± SE; 2-sided *t* test) and primary NA-ATLL and normal CD4 cells (mean ± SE; FDR-adjusted *P* value). TPM, transcripts per million. (E) *CCR4* and *ETS1* expression are highly correlated in NA-ATLL cell lines ($P < .001$; $R = 0.995$) and NA-ATLL primary cells ($P = .026$; $R = 0.662$). Pearson correlation; TPM, transcripts per million. (F) siRNA knockdown of *ETS1* resulted in decreased *CCR4* expression ($P = .021$). ATL18 cell line; 2-sided *t* test, mean ± standard deviation. Data are representative of 3 separate transfections. (G-H) *ETS1* and *CCR4* expression stratified by *CCR4* mutation status in NA-ATLL primary tumor cells. Mean ± standard deviation, 2-sided *t* test.

HTLV-1.[58,59] In addition to Tax, interactions have been reported between ETS1 and other transcription factors such as Runx1 and Notch to facilitate DNA binding.[35,44] Of note, the RUNX1 motif was also identified in NA-ATLL cell lines suggesting potential for cooperation between ETS1 and RUNX1 in this context. Further work is required to investigate potential interactions between ETS1, HTLV-1 proteins, and other T-cell transcription factors, as well as role for other Ets family transcription factors.

We identified *CCR4* as a direct transcriptional target of ETS1 in NA-ATLL. This is consistent with a recent report of *CCR4* as an ETS1 target gene in T-cell acute lymphoblastic leukemia.[35] CCR4 is a chemokine receptor for ligands CCL17 and CCL22, expressed primarily on TH2 and Treg cells. CCR4 is frequently expressed in ATL[10] and is associated with poor prognosis.[60] HTLV-1 Tax has been shown to induce the CCR4 ligand, *CCL22*, in HTLV-1–infected cells, resulting in selective attraction of $CCR4^+$ T cells.[61] Both *CCR4* and *CCL22* are overexpressed in NA-ATLL compared with J-ATLL cell lines (data not shown).

HBZ-induced GATA3 has also been shown to drive *CCR4* expression in J-ATLL cells,[48] and GATA3 and CCR4 are coexpressed in PTCL.[62] Moreover, GATA3, Tax1, and ETS1/2 have been shown to interact to promote gene transcription in HTLV-1–transformed cells.[63] Both Ets and GATA3 binding motifs are abundant within the *CCR4* chromatin accessibility region. In J-ATLL primary samples and cell lines, both *ETS1* and *GATA3* are correlated with *CCR4* expression. Whereas in NA-ATLL cell lines and primary samples, *ETS1*, but not *GATA3* were correlated with *CCR4*, despite elevated GATA3 expression.

CCR4 mutations have not been previously reported for NA-ATLL as *CCR4* was not included in the original genotyping panel for this patient cohort.[8] Recurrent gain of function mutations in *CCR4* (29%) have been reported in J-ATLL and for all 4 J-ATLL cell lines used in this study.[49,50] We found a similar rate of mutation in NA-ATLL with 3 of 9 cases harboring nonsense mutations located in the C-terminal cytoplasmic region and another case with a previously uncharacterized missense mutation in the transmembrane region. Expression of the truncated mutant *CCR4* has been shown to result in decreased receptor internalization and increased migration in response to ligands.[49,50] Further work is needed to comprehensively characterize *CCR4* variant status in NA-ATLL. It is possible that ETS1-driven upregulation of *CCR4* in NA-ATLL is a way to promote CCR4 function in the absence of a gain of function mutation.

The prevalence of epigenetic mutations, in particular, *EP300*, are a differentiating feature of NA-ATLL.[8] Robust chromatin accessibility differences were not observed on the basis of *EP300* mutational status between *EP300* mutant ($n = 3$) and wild-type ($n = 5$) cell lines. However, the study was not adequately powered for this comparison.

Our finding of BATF3/IRF4 motif enrichment is consistent with a recent study showing that HBZ drove the BATF3/IRF4 transcriptional program through interactions with BATF3.[17] This study by Nakagawa et al was performed using J-ATLL cell lines, and we show the intronic HBZ interacting site identified has increased chromatin accessibility in J-ATLL cell lines compared with NA-ATLL. These findings indicate differential expression and/or regulatory relationships between transcriptional regulators and HTLV-1 viral proteins in J-ATLL and NA-ATLL.

The cause of the clinical and molecular differences between NA-ATLL and J-ATLL remains an important question. It is likely that these differences are being driven by the presence or interactions of various genetic and environmental factors. The geographic differences and specific roles of factors such as host genetic variants, HLA expression, route and timing of HTLV-1 infection, and presence of co-infections remain largely unknown and will be important to define. The role of HTLV-1 genotype is also an important consideration. Although the genetically stable Cosmopolitan subtype 1a is common in both Japan and North America, Cosmopolitan subtype 1a subgroup A (transcontinental) is dominant in North America, whereas subgroup B (Japanese) together with subgroup A are found in Japan. There is evidence that ATLL in South America, where Cosmopolitan subtype 1a subgroup A is dominant, has more aggressive clinical course and younger age of diagnosis compared with J-ATLL, although subtype distribution may favor lymphomatous rather than acute as observed in NA-ATLL.[64] Of particular interest will be characterization of ATLL in patients of Melanesian descent with the more divergent HTLV-1c genotype and patients of African descent where HTLV-1b and a spectrum of HTLV-1a subgroups are endemic.[65] It has been suggested that HTLV-1c may be less oncogenic than Cosmopolitan subtype 1a, but likely underreporting and differences in life expectancy and environmental factors, particularly in indigenous populations, have made this comparison difficult.

Despite disparate prognostic and mutation profiles, J-ATLL and NA-ATLL are treated similarly because of the limited understanding of NA-ATLL biology. Our data demonstrate that NA-ATLL has a distinct molecular profile, characterized by a key role for the transcriptional regulator, ETS1. Further work is needed to validate this chromatin signature in primary tumors and to elucidate the clinical implications and association with response to treatment, including anti-CCR4 (mogamulizumab) to help guide therapeutic approaches for NA-ATLL.

Acknowledgments

The authors thank Niraj Shenoy for generously supporting this work with his Albert Einstein Cancer Center grant and for critical reading/input and B. Hilda Ye (Albert Einstein College of Medicine) for generously sharing ATLL cell lines and primary NA-ATLL and normal T cell RNA-sequencing data.

Authorship

Contribution: R.A.L. planned the study, performed experiments, analyzed data, and wrote the manuscript; Y.Z. and S.B.M. prepared ATAC libraries; R.K.A. performed experiments; and K.P. provided sequencing data.

Conflict-of-interest disclosure: The authors declare no competing financial interests.

ORCID profiles: R.A.L., 0000-0002-7523-5010; R.K.A., 0000-0002-5693-1758.

Correspondence: Rebecca A. Luchtel, Department of Medicine (Hematology & Oncology), Northwestern University Feinberg School of Medicine, 420 E Superior St, Chicago, IL 60611; email: rebecca.luchtel@northwestern.edu.

References

1. Sandell RF, Boddicker RL, Feldman AL. Genetic landscape and classification of peripheral T cell lymphomas. *Curr Oncol Rep*. 2017;19(4):28.
2. Yamaguchi K, Watanabe T. Human T lymphotropic virus type-I and adult T-cell leukemia in Japan. *Int J Hematol*. 2002;76(suppl 2):240-245.
3. Satake M, Yamada Y, Atogami S, Yamaguchi K. The incidence of adult T-cell leukemia/lymphoma among human T-lymphotropic virus type 1 carriers in Japan. *Leuk Lymphoma*. 2015;56(6):1806-1812.
4. Shah UA, Shah N, Qiao B, et al. Epidemiology and survival trend of adult T-cell leukemia/lymphoma in the United States. *Cancer*. 2019;126(3):567-574.
5. Phillips AA, Shapira I, Willim RD, et al. A critical analysis of prognostic factors in North American patients with human T-cell lymphotropic virus type-1-associated adult T-cell leukemia/lymphoma: a multicenter clinicopathologic experience and new prognostic score. *Cancer*. 2010;116(14):3438-3446.
6. Zell M, Assal A, Derman O, et al. Adult T-cell leukemia/lymphoma in the Caribbean cohort is a distinct clinical entity with dismal response to conventional chemotherapy. *Oncotarget*. 2016;7(32):51981-51990.
7. Licata MJ, Janakiram M, Tan S, et al. Diagnostic challenges of adult T-cell leukemia/lymphoma in North America - a clinical, histological, and immunophenotypic correlation with a workflow proposal. *Leuk Lymphoma*. 2018;59(5):1188-1194.
8. Shah UA, Chung EY, Giricz O, et al. North American ATLL has a distinct mutational and transcriptional profile and responds to epigenetic therapies. *Blood*. 2018;132(14):1507-1518.
9. Malpica L, Pimentel A, Reis IM, et al. Epidemiology, clinical features, and outcome of HTLV-1-related ATLL in an area of prevalence in the United States. *Blood Adv*. 2018;2(6):607-620.
10. Yoshie O, Fujisawa R, Nakayama T, et al. Frequent expression of CCR4 in adult T-cell leukemia and human T-cell leukemia virus type 1-transformed T cells. *Blood*. 2002;99(5):1505-1511.
11. Chen S, Ishii N, Ine S, et al. Regulatory T cell-like activity of Foxp3+ adult T cell leukemia cells. *Int Immunol*. 2006;18(2):269-277.
12. Karube K, Ohshima K, Tsuchiya T, et al. Expression of FoxP3, a key molecule in CD4CD25 regulatory T cells, in adult T-cell leukaemia/lymphoma cells. *Br J Haematol*. 2004;126(1):81-84.
13. Watanabe T. Adult T-cell leukemia: molecular basis for clonal expansion and transformation of HTLV-1-infected T cells. *Blood*. 2017;129(9):1071-1081.
14. Ratner L. Molecular biology of human T cell leukemia virus. *Semin Diagn Pathol*. 2019.
15. Alasiri A, Abboud Guerr J, Hall WW, Sheehy N. Novel interactions between the human T-cell leukemia virus type 1 antisense protein HBZ and the SWI/SNF chromatin remodeling family: implications for viral life cycle. *J Virol*. 2019;93(16):e00412-19.
16. Lemasson I, Polakowski NJ, Laybourn PJ, Nyborg JK. Transcription factor binding and histone modifications on the integrated proviral promoter in human T-cell leukemia virus-I-infected T-cells. *J Biol Chem*. 2002;277(51):49459-49465.
17. Nakagawa M, Shaffer AL III, Ceribelli M, et al. Targeting the HTLV-I-regulated BATF3/IRF4 transcriptional network in adult T cell leukemia/lymphoma. *Cancer Cell*. 2018;34(2):286-297.e10.
18. Chung EY, Mai Y, Shah UA, et al. PAK kinase inhibition has therapeutic activity in novel preclinical models of adult T-cell leukemia/lymphoma. *Clin Cancer Res*. 2019;25(12):3589-3601.
19. Maeda M, Tanabe-Shibuya J, Miyazato P, et al. IL-2/IL-2 Receptor Pathway Plays a Crucial Role in the Growth and Malignant Transformation of HTLV-1-Infected T Cells to Develop Adult T-Cell Leukemia. *Front Microbiol*. 2020;11:356.
20. Corces MR, Trevino AE, Hamilton EG, et al. An improved ATAC-seq protocol reduces background and enables interrogation of frozen tissues. *Nat Methods*. 2017;14(10):959-962.
21. Calderon D, Nguyen MLT, Mezger A, et al. Landscape of stimulation-responsive chromatin across diverse human immune cells. *Nat Genet*. 2019;51(10):1494-1505.
22. Langmead B, Salzberg SL. Fast gapped-read alignment with Bowtie 2. *Nat Methods*. 2012;9(4):357-359.
23. Li H, Handsaker B, Wysoker A, et al; 1000 Genome Project Data Processing Subgroup. The sequence alignment/map format and SAMtools. *Bioinformatics*. 2009;25(16):2078-2079.
24. Zhang Y, Liu T, Meyer CA, et al. Model-based analysis of ChIP-Seq (MACS). *Genome Biol*. 2008;9(9):R137.
25. Stark R, Brown GD. DiffBind: differential binding analysis of ChIP-seq peak data. Bioconductor. Accessed 10 February 2020. http://bioconductor.org/packages/release/bioc/html/DiffBind.html
26. Bailey TL, Boden M, Buske FA, et al. MEME SUITE: tools for motif discovery and searching. *Nucleic Acids Res*. 2009;37(Web Server issue):W202-W208.
27. Machanick P, Bailey TL. MEME-ChIP: motif analysis of large DNA datasets. *Bioinformatics*. 2011;27(12):1696-1697.
28. Gupta S, Stamatoyannopoulos JA, Bailey TL, Noble WS. Quantifying similarity between motifs. *Genome Biol*. 2007;8(2):R24.
29. Fujikawa D, Nakagawa S, Hori M, et al. Polycomb-dependent epigenetic landscape in adult T-cell leukemia. *Blood*. 2016;127(14):1790-1802.
30. Yamagishi M, Nakano K, Miyake A, et al. Polycomb-mediated loss of miR-31 activates NIK-dependent NF-κB pathway in adult T cell leukemia and other cancers. *Cancer Cell*. 2012;21(1):121-135.

31. Wang X, Dasari S, Nowakowski GS, et al. Retinoic acid receptor alpha drives cell cycle progression and is associated with increased sensitivity to retinoids in T-cell lymphoma. *Oncotarget*. 2017;8(16):26245-26255.
32. Subramanian A, Tamayo P, Mootha VK, et al. Gene set enrichment analysis: a knowledge-based approach for interpreting genome-wide expression profiles. *Proc Natl Acad Sci USA*. 2005;102(43):15545-15550.
33. Rouillard AD, Gundersen GW, Fernandez NF, et al. The harmonizome: a collection of processed datasets gathered to serve and mine knowledge about genes and proteins. *Database (Oxford)*. 2016;2016:baw100.
34. Matys V, Fricke E, Geffers R, et al. TRANSFAC: transcriptional regulation, from patterns to profiles. *Nucleic Acids Res*. 2003;31(1):374-378.
35. McCarter AC, Della Gatta G, Melnick A, et al. Combinatorial ETS1-dependent control of oncogenic NOTCH1 enhancers in T-cell leukemia. *Blood Cancer Discov*. 2020;1(2):178-197.
36. Schmidl C, Hansmann L, Lassmann T, et al; FANTOM consortium. The enhancer and promoter landscape of human regulatory and conventional T-cell subpopulations. *Blood*. 2014;123(17):e68-e78.
37. Hollenhorst PC, Chandler KJ, Poulsen RL, Johnson WE, Speck NA, Graves BJ. DNA specificity determinants associate with distinct transcription factor functions. *PLoS Genet*. 2009;5(12):e1000778.
38. Wang J, Dai X, Berry LD, Cogan JD, Liu Q, Shyr Y. HACER: an atlas of human active enhancers to interpret regulatory variants. *Nucleic Acids Res*. 2019;47(D1):D106-D112.
39. Andersson R, Gebhard C, Miguel-Escalada I, et al. An atlas of active enhancers across human cell types and tissues. *Nature*. 2014;507(7493):455-461.
40. Liu W, Xie Y, Ma J, et al. IBS: an illustrator for the presentation and visualization of biological sequences. *Bioinformatics*. 2015;31(20):3359-3361.
41. Boddicker RL, Kip NS, Xing X, et al. The oncogenic transcription factor IRF4 is regulated by a novel CD30/NF-κB positive feedback loop in peripheral T-cell lymphoma. *Blood*. 2015;125(20):3118-3127.
42. Tsao HW, Tai TS, Tseng W, et al. Ets-1 facilitates nuclear entry of NFAT proteins and their recruitment to the IL-2 promoter. *Proc Natl Acad Sci USA*. 2013;110(39):15776-15781.
43. Subramanian VS, Sabui S, Moradi H, Marchant JS, Said HM. Inhibition of intestinal ascorbic acid uptake by lipopolysaccharide is mediated via transcriptional mechanisms. *Biochim Biophys Acta Biomembr*. 2018;1860(2):556-565.
44. Gu TL, Goetz TL, Graves BJ, Speck NA. Auto-inhibition and partner proteins, core-binding factor beta (CBFbeta) and Ets-1, modulate DNA binding by CBFalpha2 (AML1). *Mol Cell Biol*. 2000;20(1):91-103.
45. Testoni M, Chung EY, Priebe V, Bertoni F. The transcription factor ETS1 in lymphomas: friend or foe? *Leuk Lymphoma*. 2015;56(7):1975-1980.
46. Kato T, Fujita Y, Nakane K, et al. ETS1 promotes chemoresistance and invasion of paclitaxel-resistant, hormone-refractory PC3 prostate cancer cells by up-regulating MDR1 and MMP9 expression. *Biochem Biophys Res Commun*. 2012;417(3):966-971.
47. Khanna A, Mahalingam K, Chakrabarti D, Periyasamy G. Ets-1 expression and gemcitabine chemoresistance in pancreatic cancer cells. *Cell Mol Biol Lett*. 2011;16(1):101-113.
48. Sugata K, Yasunaga J, Kinosada H, et al. HTLV-1 viral factor HBZ induces CCR4 to promote T-cell migration and proliferation. *Cancer Res*. 2016;76(17):5068-5079.
49. Nakagawa M, Schmitz R, Xiao W, et al. Gain-of-function CCR4 mutations in adult T cell leukemia/lymphoma. *J Exp Med*. 2014;211(13):2497-2505.
50. Kataoka K, Nagata Y, Kitanaka A, et al. Integrated molecular analysis of adult T cell leukemia/lymphoma. *Nat Genet*. 2015;47(11):1304-1315.
51. Mouly E, Chemin K, Nguyen HV, et al. The Ets-1 transcription factor controls the development and function of natural regulatory T cells. *J Exp Med*. 2010;207(10):2113-2125.
52. Dittmer J. The biology of the Ets1 proto-oncogene. *Mol Cancer*. 2003;2(1):29.
53. Watanabe M, Itoh K, Togano T, et al. Ets-1 activates overexpression of JunB and CD30 in Hodgkin's lymphoma and anaplastic large-cell lymphoma. *Am J Pathol*. 2012;180(2):831-838.
54. Ren YL, Nong L, Zhang S, Zhao J, Zhang XM, Li T. Analysis of 142 Northern Chinese patients with peripheral T/NK-Cell lymphomas: subtype distribution, clinicopathologic features, and prognosis. *Am J Clin Pathol*. 2012;138(3):435-447.
55. Boxus M, Twizere JC, Legros S, Dewulf JF, Kettmann R, Willems L. The HTLV-1 Tax interactome. *Retrovirology*. 2008;5(1):76.
56. Dittmer J, Pise-Masison CA, Clemens KE, Choi KS, Brady JN. Interaction of human T-cell lymphotropic virus type I Tax, Ets1, and Sp1 in transactivation of the PTHrP P2 promoter. *J Biol Chem*. 1997;272(8):4953-4958.
57. Dittmer J, Gitlin SD, Reid RL, Brady JN. Transactivation of the P2 promoter of parathyroid hormone-related protein by human T-cell lymphotropic virus type I Tax1: evidence for the involvement of transcription factor Ets1. *J Virol*. 1993;67(10):6087-6095.
58. Bosselut R, Duvall JF, Gégonne A, et al. The product of the c-ets-1 proto-oncogene and the related Ets2 protein act as transcriptional activators of the long terminal repeat of human T cell leukemia virus HTLV-1. *EMBO J*. 1990;9(10):3137-3144.
59. Gitlin SD, Dittmer J, Shin RC, Brady JN. Transcriptional activation of the human T-lymphotropic virus type I long terminal repeat by functional interaction of Tax1 and Ets1. *J Virol*. 1993;67(12):7307-7316.
60. Ishida T, Utsunomiya A, Iida S, et al. Clinical significance of CCR4 expression in adult T-cell leukemia/lymphoma: its close association with skin involvement and unfavorable outcome. *Clin Cancer Res*. 2003;9(10 Pt 1):3625-3634.

61. Hieshima K, Nagakubo D, Nakayama T, Shirakawa AK, Jin Z, Yoshie O. Tax-inducible production of CC chemokine ligand 22 by human T cell leukemia virus type 1 (HTLV-1)-infected T cells promotes preferential transmission of HTLV-1 to CCR4-expressing CD4+ T cells. *J Immunol*. 2008;180(2):931-939.

62. Amador C, Greiner TC, Heavican TB, et al. Reproducing the molecular subclassification of peripheral T-cell lymphoma-NOS by immunohistochemistry. *Blood*. 2019;134(24):2159-2170.

63. Blumenthal SG, Aichele G, Wirth T, Czernilofsky AP, Nordheim A, Dittmer J. Regulation of the human interleukin-5 promoter by Ets transcription factors. Ets1 and Ets2, but not Elf-1, cooperate with GATA3 and HTLV-I Tax1. *J Biol Chem*. 1999;274(18):12910-12916.

64. Malpica L, Enriquez DJ, Castro DA, et al. Real-world data on adult t-cell leukemia/lymphoma in Latin America: a study from the Grupo de Estudio Latinoamericano de Linfoproliferativos. *JCO Glob Oncol*. 2021;7(7):1151-1166.

65. Afonso PV, Cassar O, Gessain A. Molecular epidemiology, genetic variability and evolution of HTLV-1 with special emphasis on African genotypes. *Retrovirology*. 2019;16(1):39.